

Exploiting Locally Imposed Anisotropies in (Ga,Mn)As: a Non-volatile Memory Device

K. Pappert, S. Hümpfner, C. Gould, J. Wenisch, K. Brunner, G. Schmidt, and L.W. Molenkamp
Physikalisches Institut (EP3), Universität Würzburg, Am Hubland, D-97074 Würzburg, Germany

(Dated: February 6, 2008)

Progress in (Ga,Mn)As lithography has recently allowed us to realize structures where unique magnetic anisotropy properties can be imposed locally in various regions of a given device. We make use of this technology to fabricate a device in which we study transport through a constriction separating two regions whose magnetization direction differs by 90° . We find that the resistance of the constriction depends on the flow of the magnetic field lines in the constriction region and demonstrate that such a structure constitutes a non-volatile memory device.

(Ga,Mn)As can be regarded as a prototypical material for investigating potential device applications of ferromagnetic semiconductors. The spin-orbit mediated coupling of magnetic and semiconductor properties in this material gives rise to many novel transport-related phenomena which can be harnessed for device applications. Previously reported device concepts include strong anisotropic magnetoresistance (AMR), in-plane Hall effect [1], tunneling anisotropic magnetoresistance (TAMR) [2, 3, 4] and Coulomb blockade AMR[5]. These previous demonstrations have been based on structures which have the same magnetic properties, inherited from the unstructured (Ga,Mn)As layer, throughout the device. Improvement in lithographic capabilities [6] has recently allowed for the first time the production of structures where distinct anisotropies are imposed locally to various functional elements of the same device by overwriting the parent layer anisotropy. This greatly enhances the scope of possible device paradigms open to investigation as it allows for devices where the functional element involves transport between regions with different magnetic anisotropy properties.

In this letter we present the first such device. It is comprised of two (Ga,Mn)As nanobars, oriented perpendicular to each other, and with each nanobar exhibiting strong uniaxial magnetic anisotropy. These two nanobars are electrically connected through a constriction whose resistance is determined by the relative magnetization states of the nanobars. We show that the anisotropic magnetoresistance effect yields different constriction resistances depending on the relative orientation of the two nanobar-magnetization vectors. The structure can thus be viewed as the basis of a ferromagnetic semiconductor memory device that operates in the non-volatile regime.

For the device, we use a 20 nm thick (Ga,Mn)As layer grown on a GaAs substrate [7] by low-temperature molecular beam epitaxy. Using an electron-beam lithography(EBL) defined Ti-mask and chemically assisted ion beam etching (CAIBE) this layer is patterned into several pairs of coupled nanobars[6] as shown in the SEM micrograph in Fig. 1. Ti/Au contacts are defined in another EBL-step through metal evaporation and lift-off, yielding resistance area products of $\sim 1\mu\Omega\text{cm}^2$. The bars are circa 200 nm wide and 1 μm long and oriented along the

[100] and [010] crystal direction, respectively. They form a 90° -angle and touch each other in one corner, where a constriction with a width of some tens of nm is formed.

Transport measurements are carried out at 4 K in a magnetocryostat fitted with a vector field magnet that allows the application of a magnetic field of up to 300 mT in any direction. The sample state is first "written" by an in-plane magnetic field of 300 mT along a writing angle φ (as defined in Fig. 1). The field is then slowly swept back to zero while ensuring that the magnetic field vector never deviates from the φ -direction. We measure the four-terminal resistance of the constriction in the resulting remanent state by applying a voltage V_b to the current leads (I_+ and I_-), and recording both the voltage drop between contacts V_+ and V_- and the current that is flowing from I_+ to I_- (Fig. 1). The polar plot of Fig. 2 shows the constriction resistance of the remanent magnetization state as a function of the writing angle φ . The resistance, which is dominated by the constriction, has a higher value upon writing the sample in the (extended) first quadrant ($-3^\circ \leq \varphi < 98^\circ$) and a lower value upon writing in the (shrunken) second quadrant ($98^\circ < \varphi < 167^\circ$). As a whole the plot is point-symmetric with respect to the origin.

To explain these results, we first examine the behav-

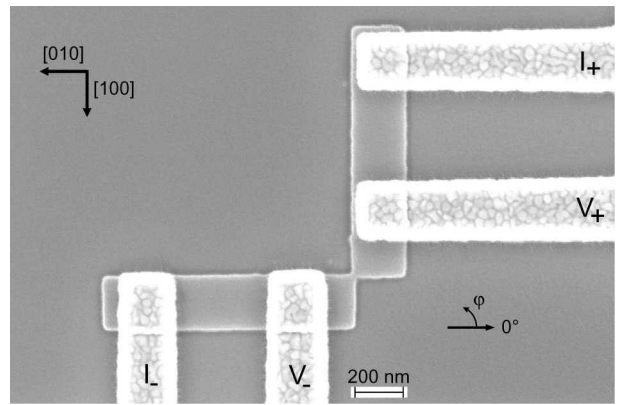


FIG. 1: SEM photograph of the device identifying the orientation of the nanobars with respect to the crystal directions, and the definition of the current (I_+, I_-) and voltage (V_+, V_-) leads and the writing angle φ

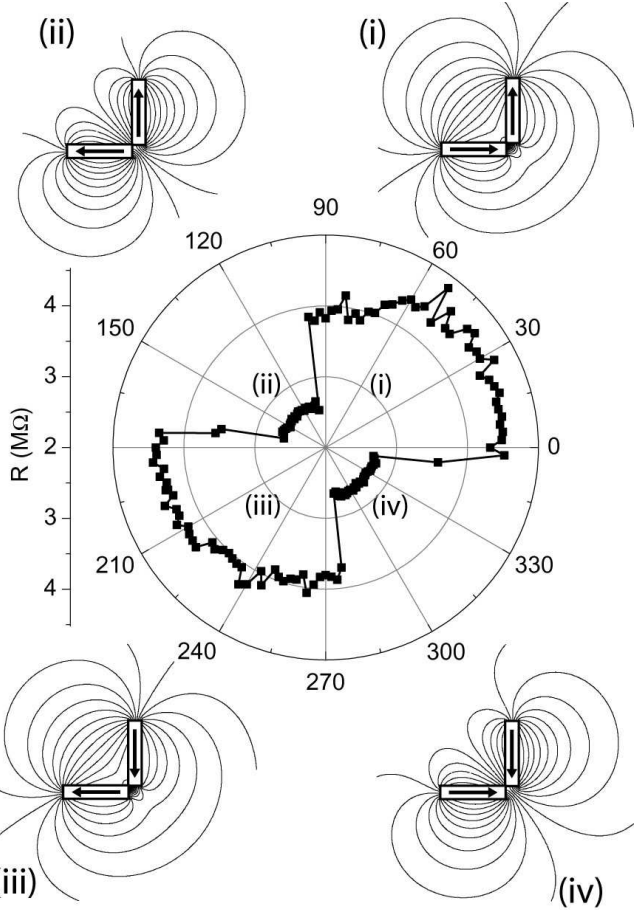


FIG. 2: Polar plot showing the results of a "write-read" experiment. The state of the device is written by applying a magnetic field of 300 mT in the φ direction. This field is then swept back to zero, and the resistance of the device is measured. The insets sketch the magnetic configuration of the device in each quadrant and the corresponding field line patterns[15].

ior of the individual nanobars. They are patterned on the sub-micron scale to make use of anisotropic strain relaxation, which in turn causes a uniaxial magnetic anisotropy that is strong enough to overwrite the intrinsic anisotropy of the (Ga,Mn)As layer[6]. We therefore expect each nanobar to show a uniaxial magnetic anisotropy with a magnetic easy axis along the respective long axis of each of the nanobars. That this is true also for coupled nanobars is confirmed in Fig. 3, which shows two terminal magnetoresistance scans, performed separately on the 0°-nanobar (Fig. 3a) and the 90°-nanobar (Fig. 3b) pictured in Fig. 1. The plots show field sweeps from -300 to +300 mT for various in-plane field directions φ between 0° and 90°. Metallic (Ga,Mn)As exhibits a higher resistance value when the magnetization \mathbf{M} is perpendicular to the current \mathbf{J} , than when \mathbf{M} is parallel to \mathbf{J} (this is the AMR effect [8],[9]). When the field \mathbf{H} is swept along 0° (thick line in Fig. 3a), the resistance of the 0°-nanobar remains in the low state [10], indicating

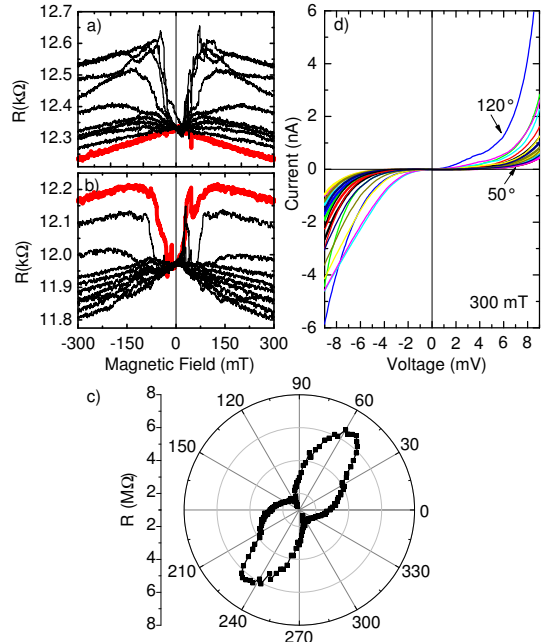


FIG. 3: Magnetoresistance measurements on the 0°(a) and 90°-nanobar(b) confirming that each exhibits a strong uniaxial magnetic anisotropy along its long axis. Field sweeps from -300 to 300 mT along 0°(thick line)...90° in 10° steps. c) Polar plot showing the resistance of the constriction in a field of 300 mT at various angles.

that \mathbf{M} is parallel to \mathbf{J} throughout the entire magnetic field range. All the other MR-scans start at a higher resistance value and merge into the low resistance curve at zero field, indicating that \mathbf{M} , which is almost parallel to \mathbf{H} at high fields, relaxes towards the 0° uniaxial easy axis as the field is decreased. Analogously, the uniaxial easy axis of the 90°-nanobar is along 90° (Fig. 3b). Consequently, the 90°-MR-scan is a flat low resistance curve. During the 0°-scan (thick line) the magnetization relaxes from parallel to the field (high resistance) towards the easy axis along the bar (low resistance) at zero field.

Given that both bars show a uniaxial magnetic easy axis along their respective long axis, the structure has four possible magnetic states at zero magnetic field as sketched in Fig. 2. In sectors (i) and (iii) the nanobars are magnetized "in series", i.e. the magnetization vectors meet in a configuration which we will call *head-to-tail*. In (ii) and (iv) on the other hand, both magnetization vectors point away from (*tail-to-tail*) or towards (*head-to-head*) the constriction. When the sample is magnetized along a given direction at 300 mT, the magnetization of both bars is almost parallel to the magnetic field. As the field is then lowered to zero, the magnetization of each nanobar relaxes to the respective nanobar easy axis, selecting the direction which is closest to the writing angle φ . For a nanobar along 0° this means, assuming no interaction between the bars, that \mathbf{M} relaxes to 0° upon writing the bar along any angle between +90° and -90°;

otherwise \mathbf{M} relaxes to 180° . If the bars in our device were non-interacting, one would thus expect the magnetization configuration in each quadrant to be as depicted in the sketches of Fig. 2, with each quadrant accounting for exactly one fourth of the total plot.

The deviation from this behavior in the actual device is due to magnetostatic interactions between the two bars, which cause a preference for head-to-tail configurations. A simple magnetostatic calculation shows that the repulsive field felt by the tip of one bar due to being near the wrong pole of the other bar is of the order of 2 mT, which is $\sim 5\%$ of the uniaxial anisotropy field. The energy density of this field is thus strong enough to overcome a small part of the energy barrier against rotation towards the opposite magnetization direction, which corresponds to an angle of $\sim 3^\circ$. The head-to-tail quadrants thus increase commensurably.

Magnetic field line patterns for the four magnetization configurations were calculated (sketches in Fig. 2i-iv) using a simple bar magnet model. The field lines are close to parallel to the current in the head-to-tail configuration (Fig. 2i and iii). In the tail-to-tail and the head-to-head configuration (Fig. 2ii and iv) the field lines are approximately perpendicular to the current.

Having understood the magnetic configuration of the device in the write-read experiment of Fig. 2, we now turn to an explanation of why these should lead to two very distinct resistance states. The above magnetostatic arguments and internal fields, in connection with the AMR coefficient for metallic (Ga,Mn)As can explain a few percent resistance difference [1, 9] between the head-to-tail and the head-to-head configuration, much smaller and of a different sign than the effect in Fig. 2. We have actually observed such a small AMR related effect in a similar structure, which has a wider constriction (100 times lower constriction resistance). Fig. 4a shows similar data on this low resistance sample as Fig. 2 for the high resistance sample. It is immediately obvious from Fig. 4a that this sample shows the same remanent magnetization configurations as the device in Fig. 2. However, the effect is much smaller and of the opposite sign: where Fig. 2 exhibits a high resistance state, Fig. 4a shows a low state, and *vice versa*.

We ascribe the difference in behavior between Figs. 2a and 4a to the occurrence of depletion in the constriction in the sample of Fig. 2a, which drives the transport (in the critical constriction region) into the hopping regime[11]. At the same time, we suggest that in the hopping regime the AMR coefficient *changes sign*, leading to the observed changes in magnetoresistance. Important evidence for this claim comes from the angle-dependent magnetoresistance behavior of the samples at a field of 300 mT, strong enough to force the magnetization close to parallel to the external field. This data is given in Fig. 3c for the high-resistance, and in Fig. 4b for the low-resistance sample.

The low-resistance device exhibits typical AMR behavior as expected for metallic (Ga,Mn)As: Fig. 4b shows

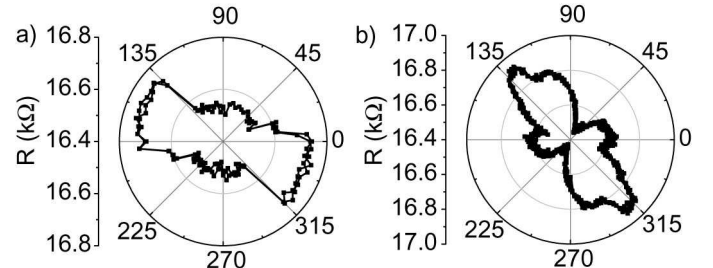


FIG. 4: (a)Results of a write-read experiment as in Fig. 2, for a device with a wider constriction, which exhibits metallic transport behavior and (b)constriction resistance in a rotating 300 mT external magnetic field.

that the resistance is lowest when \mathbf{M} is forced parallel to the current through the constriction ($\varphi \sim 45^\circ$) and ca. 3 % higher for $\mathbf{M} \perp \mathbf{J}$. In contrast, the high-resistance constriction of the device in Fig. 2 shows a huge and inverted AMR signal, as can be seen in Fig. 3c. The resistance at $\varphi \sim 45^\circ$, where $\mathbf{M} \parallel \mathbf{J}$, is more than 5 times larger than for $\mathbf{M} \perp \mathbf{J}$.

This is actually not the first observation of an inverted AMR signal; the same effect has recently been reported in thin (Ga,Mn)As devices [5, 12] in which the transport is in the hopping regime. This situation is similar to our high-resistance device, where from the resistance one already can infer that the constriction acts as a tunnel barrier. Actual evidence for tunneling transport comes from the current-voltage characteristics of the high-resistance constriction, shown in Fig. 3d, which were taken at 300 mT at different field directions φ . The I-V's are clearly non-linear, with the nonlinearity depending on the magnetization direction. Fields aligning \mathbf{M} along $\sim 120^\circ$ cause the strongest and along 50° the smallest non-linearity of the IV-curve.

The strong dependence of the IV-characteristic and the resistance on the magnetization direction are characteristic of transport going through a metal-insulator transition (MIT) from the diffusive into the hopping regime depending on the angle of the magnetization, similar to what we have previously observed in a TAMR device [4]. Such a MIT occurs in partly depleted samples due to the wave-function geometry change depending on the magnetization direction. The localized hole wave-function has an oblate shape with the smaller axis pointing in the magnetization direction ([13]). Consider the overlap of such oblate shapes statistically distributed with respect to the direction of the current in connection with the Thouless localization criterion. The wavefunction overlap is much smaller when the sample is magnetized parallel to the current, than for $\mathbf{M} \perp \mathbf{J}$, suppressing hopping transport through the depleted constriction region. This implies a magnetoresistance behavior that is exactly the inverse of that expected for the metallic regime and explains the increased resistance value in both the high field measurements (Fig. 3c along $\sim 45^\circ$) and the write-read

experiment (Fig. 2 1st quadrant).

We thus believe that our observations can be fully explained by the internal magnetic fields and the AMR coefficient as applicable to the transport regime in the constriction. A further candidate to explain our observations could be the presence of a domain wall (DW) between differently magnetized regions of the device in the head-to-head and tail-to-tail configuration, which would be absent in the head-to-tail configurations. However, since the constriction is long and the DW would not be strongly geometrically confined, one anticipates only a very low DW resistance in these samples [11, 14]. This is confirmed by a comparison of Fig. 2 with Fig. 3c: The resistance values of both remanent states in Fig. 2 are in between the extreme resistance values of the homogeneously magnetized sample. The DW contribution [11] to the constriction resistance can in the present sample thus only be a minor effect on the resistance of the remanent state and does not explain the different resistance levels in Fig. 2. [16]. In the remanent state the resistance of the head-to-head configuration, including a possible DW contribution, is lower than the resistance of the head-to-tail configuration. We can thus exclude the DW as the

origin of the two resistance states observed in Fig. 2.

In conclusion we have shown that locally imposed magnetic anisotropies in different regions of one ferromagnetic semiconductor device allow for novel device designs. We consider the perpendicularly magnetized nanobars discussed in this paper as a first demonstration of the type of devices that can be fabricated using this approach, it is certainly not difficult to conceive of further concepts in this direction. In addition, the work presented here has highlighted the difference in AMR behavior between metallic and hopping transport in (Ga,Mn)As, which again should prove useful in device design.

Acknowledgments

The authors thank M. Sawicki and M.J. Schmidt for useful discussions and V. Hock and T. Borzenko for help in sample fabrication. We acknowledge financial support from the EU (NANOSPIN FP6-IST-015728) and the German DFG (BR1960/2-2).

- [1] H. X. Tang, R.K. Kawakami, D.D. Awschalom and M.L. Roukes, Phys. Rev. Lett. **90**, 107201 (2003).
- [2] C. Gould, C. Rüster, T. Jungwirth, E. Grgis, G.M. Schott, R. Giraud, K. Brunner, G. Schmidt, and L.W. Molenkamp, Phys. Rev. Lett. **93**, 117203 (2004).
- [3] C. Rüster, C. Gould, T. Jungwirth, J. Sinova, G. M. Schott, R. Giraud, K. Brunner, G. Schmidt, and L. W. Molenkamp , Phys. Rev. Lett. **94**, 027203 (2005).
- [4] K. Pappert, M. J. Schmidt, S. Hümpfner, C. Rster, G. M. Schott, K. Brunner, C. Gould, G. Schmidt, and L. W. Molenkamp, Phys. Rev. Lett. **97**, 186402 (2006).
- [5] J. Wunderlich, T. Jungwirth, B. Kaestner, A. C. Irvine, A. B. Shick, N. Stone, K.-Y. Wang, U. Rana, A. D. Giddings, C. T. Foxon, R. P. Campion, D. A. Williams, and B. L. Gallagher, Phys. Rev. Lett., **97**, 077201 (2006).
- [6] S. Hümpfner, M. Sawicki, K. Pappert, J. Wenisch, K. Brunner, C. Gould, G. Schmidt, T. Dietl and L.W. Molenkamp, submitted, and cond-mat/0612439
- [7] For details of the growth, see G.M. Schott, G. Schmidt, G. Karczewski, L.W. Molenkamp, R. Jakielka, A. Barcz, G. Karczewski, Appl. Phys. Lett., **82**, 4678 (2003)
- [8] a) J. P. Jan, in "Solid State Physics" (Eds: F. Seitz, D. Turnbull), Academic Press Inc., New York, 1957. b) T.R. McGuire, R.I. Potter, IEEE Trans. Magn. **MAG-11**, 1018 (1975).
- [9] D.V. Baxter, D. Ruzmetov, J. Scherschligt, Y. Sasaki, X. Liu, J.K. Furdyna, C.H. Mielke, Phys. Rev. B **65**, 212407 (2002)
- [10] The remaining constant slope is caused by the isotropic MR effect as described, e.g., in F. Matsukura, M. Sawicki, T. Dietl, D. Chiba, H. Ohno, Physica E **21**, 1032 (2004).
- [11] C. Rüster, T. Borzenko, C. Gould, G. Schmidt, L.W. Molenkamp, Phys. Rev. Lett. **91**, 216602 (2003).
- [12] A.W.Rushforth, K.Vyborny, C.S.King, R.P.Campion, C.T. Foxon, T.Jungwirth and B.L.Gallagher, to be published
- [13] M.J. Schmidt, K. Pappert, C. Gould, G. Schmidt, R. Oppermann, and L.W. Molenkamp, to be published
- [14] P. Bruno, Phys. Rev. Lett. **83**, 2425 (1999).
- [15] Field line patterns calculated using Vizimag (www.vizimag.com).
- [16] In a separate experiment we have prepared a DW pinned at the smallest part of our constriction. This was accomplished using well defined field sequences and will be published elsewhere. In this case we observe a large positive DW contribution to the device resistance (as reported in [11]).